WATER RESOURCES RESEARCH, VOL. 36, NO. 6, PAGES 1403–1412, JUNE 2000

Application of a fractional advection-dispersion equation

David A. Benson
Desert Research Institute, Water Resources Center, Reno, Nevada

Stephen W. Wheatcraft
Department of Geologic Sciences, University of Nevada, Reno

Mark M. Meerschaert
Department of Mathematics, University of Nevada, Reno

Abstract. A transport equation that uses fractional-order dispersion derivatives has fundamental solutions that are Lévy's α-stable densities. These densities represent plumes that spread proportional to time$^{1/\alpha}$, have heavy tails, and incorporate any degree of skewness. The equation is parsimonious since the dispersion parameter is not a function of time or distance. The scaling behavior of plumes that undergo Lévy motion is accounted for by the fractional derivative. A laboratory tracer test is described by a dispersion term of order 1.55, while the Cape Cod bromide plume is modeled by an equation of order 1.65 to 1.8.

1. Introduction

Anomalous, or non-Fickian, dispersion has been an active area of research in the physics community since the introduction of continuous time random walks (CTRW) by *Montroll and Weiss* [1965]. These random walks extended the predictive capability of models built on the stochastic process of Brownian motion, which is the basis for the classical advection-dispersion equation (ADE). The CTRW assign a joint space-time distribution, called the transition density, to individual particle motions. When the tails are heavy enough (i.e., power law), non-Fickian dispersion results for all time scales and space scales. *Berkowitz and Scher* [1995, 1998] and *Painter et al*. [1998] provide reviews of CTRW and application to transport in fractured rock. Numerous authors have shown the equivalence between these heavy-tailed motions and transport equations that use fractional-order derivatives. The motions can be heavy-tailed, implying extremely long-term correlation and fractional derivatives in time [*Giona and Roman*, 1992; *Compte*, 1996] and/or space [e.g., *Gorenflo and Mainardi*, 1998; *Saichev and Zaslavsky*, 1997; *Benson*, 1998; *Chaves*, 1998; *Meerschaert et al*., 1999].

Second-order dispersion arises when tails of this distribution are sufficiently "thin" that relative to an observation or measurement event, time-consuming or very large motions are effectively ruled out. Typically, a sufficient number of thin-tailed motions must also be integrated before DeMoive's central limit theorem is a good assumption and before ergodicity and Fickian transport ensue. During this pre-Fickian phase of transport, scale-dependent dispersion coefficients can be used in a local ADE, although a nonlocal formulation is a more accurate model of these motions [*Neuman*, 1993; *Cushman et al*., 1994]. Solutions of certain nonlocal equations are gained via fast Fourier and Laplace transforms for relatively homogeneous media [e.g., *Deng et al*., 1993].

Paper number 2000WR900031.
0043-1397/00/2000WR900031$09.00

The classical ADE with a local (or asymptotically constant) dispersion tensor is a very handy predictive equation, since solutions are easily gained. The fractional-order forms of the ADE are similarly useful. General nonlocal forms of the second-order ADE are less so, since solutions must be gained by numerical convolution. Similarly, explicit numerical modeling by generation of random K fields and subsequent Monte Carlo simulation is a very time-consuming process that is commonly used to gain information about a plume's pre-Fickian behavior. The fractional ADE used herein is spatially nonlocal and models particles that experience very large transitions. The large transitions may arise from high heterogeneity [*Benson et al*., 2000] and very long spatial autocorrelation [*Benson*, 1998]. If the transition probabilities follow a power law, then analytic solutions of the fractional ADE may serve as good stand-alone models of transport throughout a plume's development. In this study we examine whether the fractional-order ADE is also a useful model for transport in relatively homogeneous material.

2. Evidence of Fractional, or α-Stable, Behavior in Relatively Homogeneous Material

The fractional ADE predicts concentration versus time and distance in closed form, once the scaled α-stable density (fundamental solution) is known. In this spirit, two experiments are analyzed in the simplest way possible to look for evidence of non-Fickian, heavy-tailed, behavior. A typical question that a contaminant hydrogeologist wishes to answer is How far and how fast will a tracer move? As a first approximation, this reduces most problems to one spatial dimension (one-dimensional (1-D)). The following experiments will be treated as such. The questions associated with multiple dimensions and averaging are left for future work.

Two experiments are analyzed in this section. The first one was intuitively expected to follow Fick's law. It is a 1-D tracer test in a laboratory-scale (1 m) sandbox. The sandbox was constructed with very uniform sand in an effort to minimize heterogeneity. The second test uses data collected by the U.S.

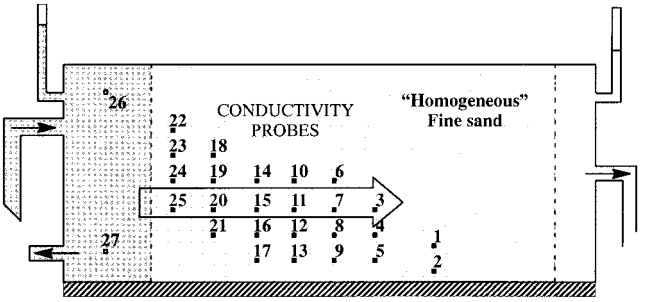

Figure 1. Schematic view of the experimental sandbox tracer tests [after *Burns*, 1996]. The flow path highlighted by the arrow is analyzed in detail.

Geological Survey during a 511-day tracer test within a relatively uniform sand-and-gravel aquifer on Cape Cod.

Since we analyze these tracer tests in one dimension, we use the 1-D form of the fractional advection-dispersion equation [*Meerschaert et al*., 1999]:

$$\frac{\partial C}{\partial t} = -v\,\frac{\partial C}{\partial x} + \mathcal{D}p\,\frac{\partial^{\alpha} C}{\partial x^{\alpha}} + \mathcal{D}(1-p)\,\frac{\partial^{\alpha} C}{\partial(-x)^{\alpha}}, \qquad (1)$$

where C is the expected concentration, t is time, v is a constant mean velocity, x is distance in the direction of mean velocity, $\mathcal{D}$ is a constant dispersion coefficient, $0 \le p \le 1$ describes the skewness of the transport process, and α is the order of fractional differentiation (appendix). For a discussion of this equation, see *Benson et al*. [2000] or *Meerschaert et al*. [1999]. When $\alpha = 2$, the dispersion operators are identical and the classical ADE is recovered. Fundamental (Green function) solutions are Lévy's α-stable densities (appendix).

2.1. Laboratory-Scale Tracer Test

A laboratory-scale sandbox (Figure 1) was constructed for the purpose of studying *Henry*'s [1964] seawater intrusion problem. The sandbox was designed and built using as homogeneous a porous medium as possible [*Burns*, 1996] for comparison to analytical solutions. Numerous researchers have shown that it is extremely difficult, if not impossible, to create a homogeneous sandbox. A number of simple tracer tests were conducted to estimate the transport characteristics of the sand. These tracer tests showed non-Gaussian breakthrough curves [*Burns*, 1996] with sigmoid shape on probability plots and heavy leading and trailing edges (tails) similar to theoretical α-stable solutions (Figure 2).

In a typical 1-D laboratory tracer test, the velocity is held constant and large enough to neglect molecular dispersion. The classical ADE is used to model the breakthrough curve using the 1-D velocity-dependent dispersion coefficient $\mathcal{D} = va_L$, where a_L is the longitudinal dispersivity. Fickian transport refers to transport within a medium in which a_L remains a constant throughout a plume's history, yielding a constant coefficient on the second-order dispersion term. This would be expected for transport at larger than pore scales in a column (or sandbox) of perfectly mixed, homogeneous sand [*Taylor*, 1953; *de Josselin de Jong*, 1958]. A continuous tracer has a breakthrough curve that is a shifted Gaussian distribution function. The curves are translated by a distance vt, which is the mean travel distance within the column. The quantity $(2a_L vt)^{1/2}$ is analogous to the standard deviation of the graph of the concentration versus distance, so the distance (X_c) between any two quantiles, or relative concentration levels, in a plume grows proportional to $(a_L t)^{1/2}$. If the rate of growth is faster, then a_L is made to absorb the increase since the second-order diffusion equation can only afford growth proportional to $t^{1/2}$.

In an α-stable plume following (1), X_c should grow proportional to $t^{1/\alpha}$. If the dispersivity is thought to grow as a power function of the mean travel distance or time during a constant velocity test (i.e., $a_L \propto t^m$), then the value of the Lévy index (α) can be directly calculated:

$$(a_L t)^{1/2} \propto (t^m t)^{1/2} \propto X_c \propto t^{1/a}. \qquad (2)$$

Some algebra gives the expression for α in terms of the slope (m) of the increase of apparent dispersivity versus time on a log-log graph: $\alpha = 2/(m+1)$. The Fickian result is recovered if the dispersivity does not increase with scale. Then $m = 0$ and $\alpha = 2$.

A series of conservative tracer tests were conducted in the sandbox to estimate the anticipated single value of a_L for the sandbox [*Burns*, 1996]. The value of dispersivity at each of 23 conductivity probes was markedly different, with a general increase of the values with mean travel distance (Figure 3). The mean travel velocity was found to decrease with depth within the sandbox, indicating the presence of fining-upward sequences and compaction that were created during sand emplacement. These sequences are not visible because of the high degree of sand uniformity [*Burns*, 1996]. The initial indication of α-stable transport within the sandbox lies within the heavy-tailed breakthrough curves (Figure 2). When the concentration is normalized and plotted on a probability axis versus scaled

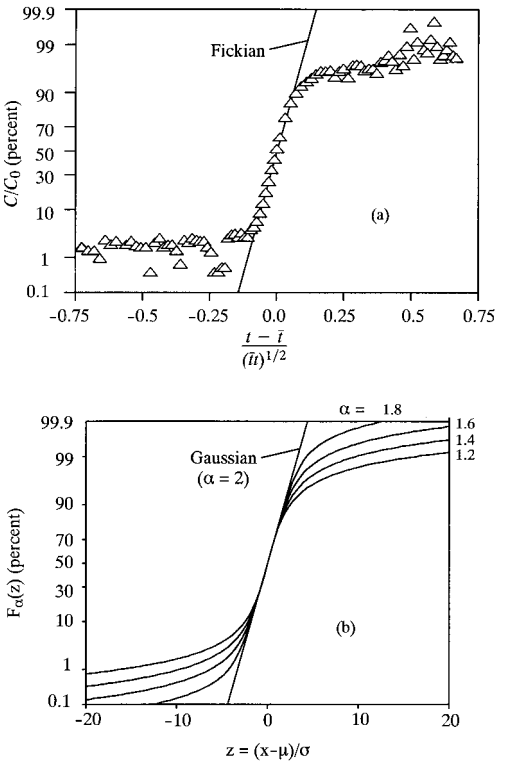

Figure 2. (a) Normalized concentration versus scaled time for probe 20, test 3 [after *Burns*, 1996]. A best fit line (implying an underlying Gaussian profile) is typically used to calculate the apparent dispersivity. (b) The α-stable distributions, which are solutions to (1) for a constant source.

time (or distance) on a normal axis, a Gaussian plume appears as a straight line [*Pickens and Grisak*, 1981]. The slope of the line is proportional to a_L, so this method is commonly used to estimate the dispersivity of the transport medium. An α-stable plume plotted in the same manner will appear nearly Gaussian throughout the middle of the breakthrough curve but will also show higher tail probabilities, presenting a sigmoid shape throughout the breakthrough curve (Figure 2). The heavy-tailed breakthrough curves are well within the probe calibration ranges [*Burns*, 1996] and cannot be attributed to instrument error.

This heavy-tailed breakthrough is typically explained and subsequently modeled by kinetic reactions or multiple compartments, or phases, into which the solute can partition [*Coats and Smith*, 1964; *van Genuchten and Wierenga*, 1976; *Brusseau et al*., 1989; *Haggerty and Gorelick*, 1995]. The compartments can be given different rates of Gaussian transport; a zero-velocity (immobile) phase is commonly used. These mobile/immobile models can be tuned to provide excellent data fits and in some cases are based on a truly immobile (i.e., dead-end pore) phase. To model skewed, heavy-tailed plumes, these theories require one or more generally empirical parameters in the form of transfer coefficients or distributions of coefficients [*Li et al*., 1994; *Haggerty and Gorelick*, 1995; *Haggerty et al*., 1998]. These methods are typically used to explain long-tailed trailing edges but do not account for non-Gaussian fast pathways. An interesting and open question is whether the heavy-tailed and possibly skewed plumes predicted by the fractional ADE can reproduce a range of results from these multiphase Gaussian models. In the sandbox, heavy leading and tailing tails are likely due to channeling within small fining-upward sequences that resulted from sand emplacement through standing water and from cracked and intact surface clays on the sand particles (Figure 4).

Each dispersivity value is difficult to estimate accurately because of the sigmoid breakthrough curves (Figure 2). The choice of dispersivity depends on a judgement of the number of data assumed to fall along a straight line. These estimates only give a rough idea of the non-Fickian growth rate of the solute pulse. We model the flow path indicated by the arrow in Figure 1 because it represents the longest flow path with six sample ports, providing six dispersivity values (Figure 3). The rest of the dispersivity data (Figure 3) are indicative of other pathways through the sandbox. Since we are using breakthrough curve data from the flow path, or stream tube, indicated in Figure 1, our comparisons are self-consistent. Our purpose here is to look for non-Fickian, heavy-tailed, behavior in this experiment. A complete analysis of the sandbox breakthrough curve data, including lateral transport, is left for further analysis.

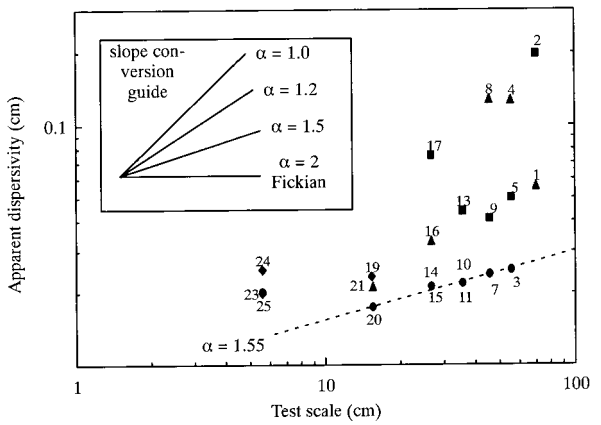

Figure 3. Calculated dispersivities versus distance of probe from source. Probes along the flow path chosen for analysis are indicated by solid ovals. The best fit dashed line indicates a fractional index (α) of 1.55.

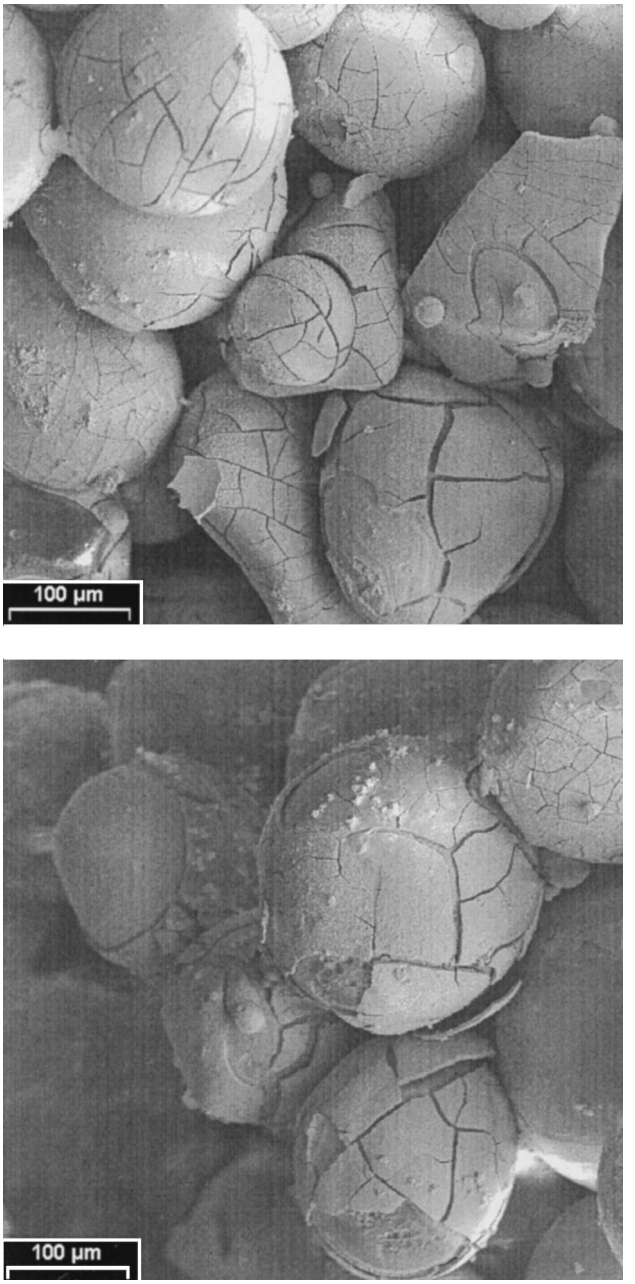

Figure 4. Photomicrographs of the sand used in *Burns*' [1996] experiment.

The apparent dispersivities along the chosen flow path indicate a value of $\alpha = 1.55$. As a result, the breakthrough curves along this flow path should be scale-invariant after shifting by the mean travel time and dividing by $t^{1/1.55}$. By plotting the tails of the distribution, i.e., C/C_0 for the leading edge and $(1.0 - C/C_0)$ for the trailing edge, versus the absolute value of $(t - t_{\text{mean}})$, the skewness and heavy, power law tails of the

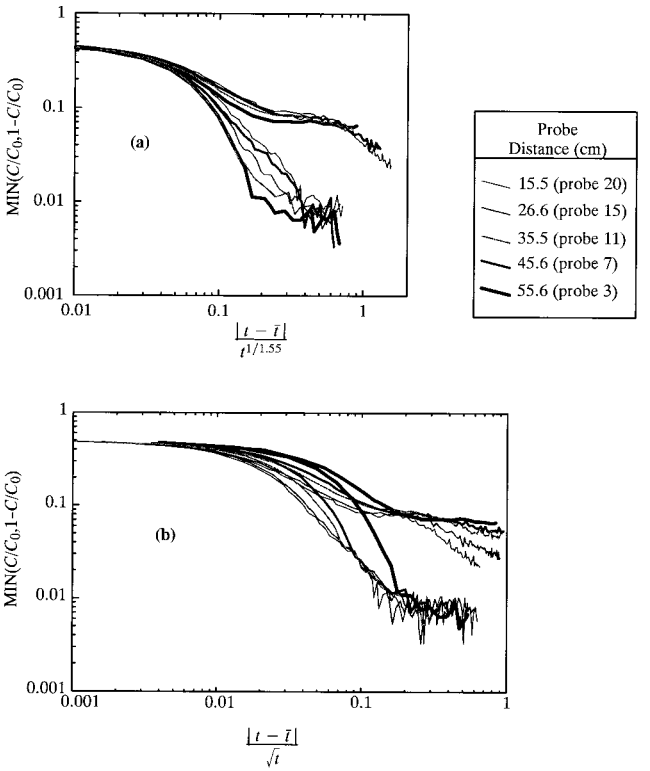

Figure 5. Measured breakthrough "tails" at probes along the flow path (a) properly rescaled by $t^{1/1.55}$ and (b) rescaled by the traditional $t^{1/2}$. Note the strong skewness that separates the leading and trailing limbs of the plume. Very early and late data show probe noise.

plume are immediately apparent (Figure 5). Proper time rescaling by $t^{1/\alpha}$ shows reasonably good agreement throughout the entire breakthrough curve history, particularly the trailing edge. One can empirically estimate the value of α by plotting the breakthrough curves with the abscissa scaled by different values of $t^{1/\alpha}$. If α is too large, the downstream curves plot to the right (Figure 5b). Too small a value of α results in downstream curves shifted to the left.

Once the index of differentiation is known, a predictive model of transport is obtained. One need only generate a single density (or distribution function for a continuous tracer test) and scale this density for any time or distance. The value of $\mathcal{D}$ is obtained from the scaling of the breakthrough curves relative to a standard α-stable curve (appendix). Several standard densities using $\alpha = 1.55$ and various skewness parameters (p) were generated to achieve the observed separation of the leading and trailing tails. A value of $p = 3/4$ provides a reasonable separation (Figure 6). Compared to the classical ADE solution, the fractional ADE model more accurately represents the heavy tails observed at all of the probe locations along the streamtube. A scale-dependent dispersivity is not needed since the fractional derivative describes the faster than Fickian transition zone growth.

2.2. Cape Cod Aquifer

In July 1985, ~7.6 m^3 of tracer was introduced into a sand and gravel aquifer in Cape Cod, Massachusetts. The injected tracer contained 640 mg/L of the relatively nonreactive bromide (Br^-) ion, as well as reactive (sorbing) Li^+ and MoO_4^{2-} ions. *LeBlanc et al.* [1991] and *Garabedian et al.* [1991] document the tracer test and the characteristics of the plume, such as estimated first and second moments. Over 650 multilevel samplers (MLS) were installed to monitor the plume (Figure 7) for over 511 days. The Br^- plume extended well beyond the MLS array after 511 days, creating an effective time cutoff for analysis of the nonreactive plume. Each MLS (the numerous small circles in Figure 7) consisted of 15 sampling ports at different depths, resulting in the collection of a large number of data points in x-y-z time coordinates.

For simplicity, the positive x direction will refer to the mean plume movement direction of roughly 8° east of south (Figure 7). The deviations that the plume made from this line are small enough that the difference between the actual travel distance and the distance projected onto this x axis is negligible. A plume of nonreactive tracer is a 3-D joint density. Analysis can be reduced to one dimension in several ways. Cross-sectional averaging investigates marginal 1-D densities. Examining the peak concentration along the plume core investigates conditional densities. Both methods suffer from various sampling, bias, and interpolation errors. We choose to analyze the plume's core, which is not mass conserving when transverse dispersion is large. However, the analysis is very simple to perform, and the peak concentrations will suffer the least amount of variability [*Kapoor and Gelhar*, 1994]. Since transverse dispersion at Cape Cod is relatively small, we examine the core by first reducing the 15 vertical samples at each MLS into a single piece of data: the maximum concentration. This maximum concentration will be considered the true peak con-

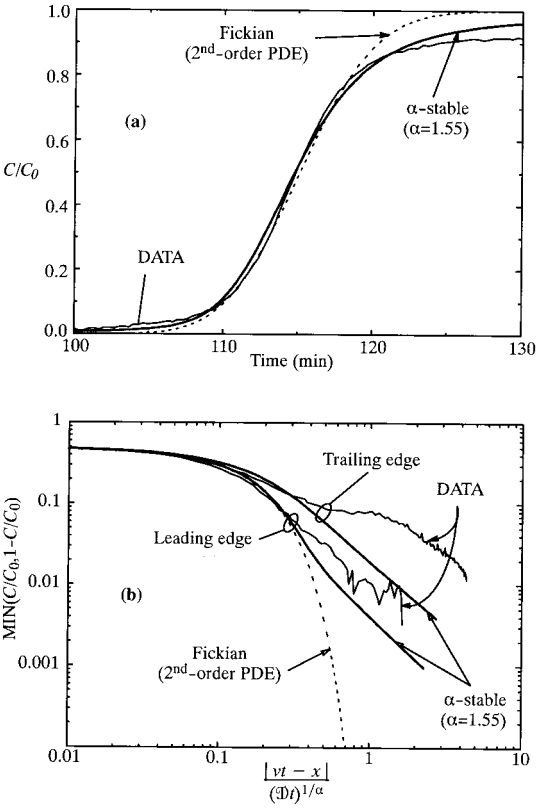

Figure 6. Comparison of traditional and fractional ADEs with the data from probe 3 ($x = 55$ cm) in the sandbox test: (a) real time and (b) data tails. Note the large underprediction of concentration by the traditional ADE at very early and late time.

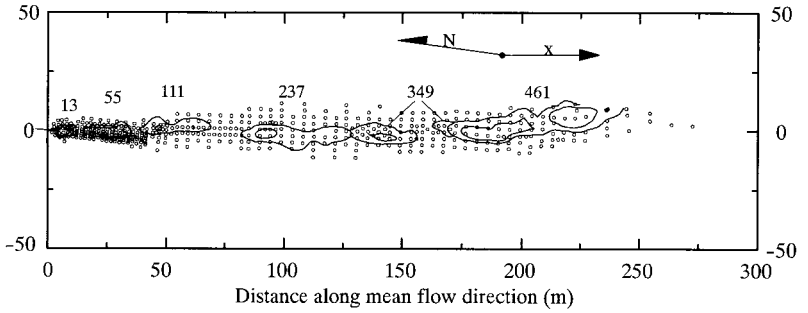

Figure 7. Aerial view of the Cape Cod Br^- plume. The plume deviated from travelling due south by ~8° to the east. Circles are multilevel samplers (MLSs).

centration at a given point in horizontal space; thus the 3-D problem is reduced to 2-D. The behavior of vertical averages at Cape Cod were very similar to these maxima [*Benson*, 1998], so we look only at the maxima here. Finally, since the MLS array generally consists of a series of MLS arranged perpendicular to the flow to laterally bracket the plume (Figure 7), the maximum concentration observed within a specific travel distance range is taken to represent the peak concentration for that distance. This procedure gives a 1-D picture of the plume at any sampling time. The peak concentrations in 3-D are projected to the x axis, resulting is a series of 1-D snapshots of the plume's core.

2.2.1. Estimation of parameters. *Garabedian et al.* [1991] calculated the variance of the plume roughly along the direction of mean travel and concluded that the growth was linear after 83 days, suggesting that a local, Fickian (second-order) governing equation is applicable after this point. A plot of the variance versus mean travel distance ($\bar{x}$) on log-log axes indicates that the growth appears nonlinear for much, if not all, of the plume's history (Figure 8), suggesting that a fractional approach may be applied. Fits of the power law and Fickian (linear) models are similar in untransformed coordinates (Figures 8a and 9a). The major difference between the plume sizes

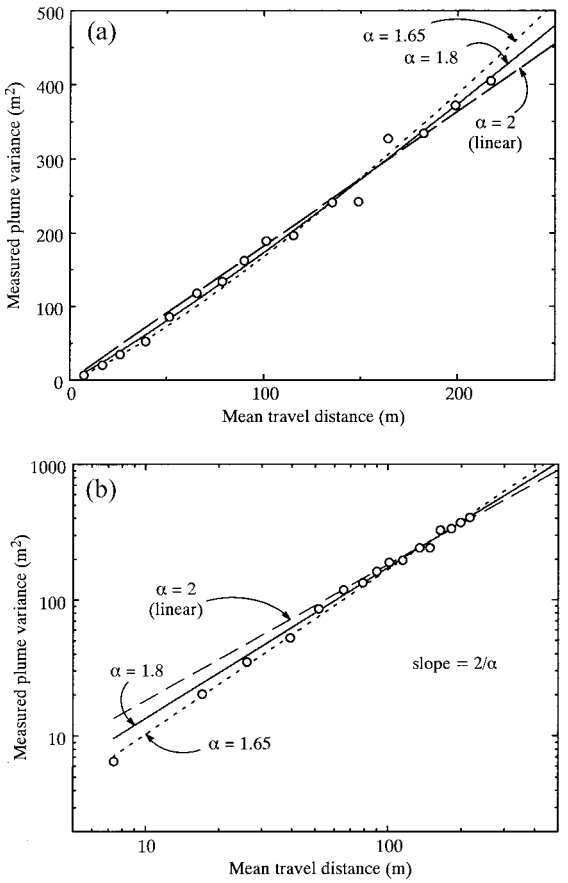

Figure 8. Calculated plume variance [*Garabedian et al.*, 1991] versus mean travel distance: (a) linear coordinates, with residuals minimized by power law with $\alpha = 1.8$; (b) log-log coordinates, showing best fit line of $\alpha = 1.65$. All lines use a zero-variance intercept.

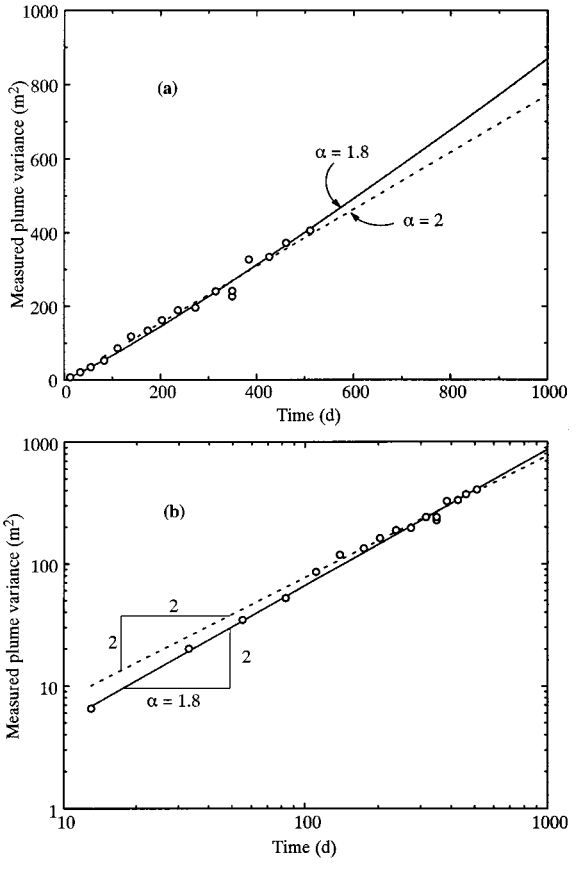

Figure 9. Calculated plume variance [*Garabedian et al.*, 1991] versus elapsed transport time: (a) linear coordinates, with roughly equal residual squared errors between data and linear or $\alpha = 1.8$ power law models; and (b) log-log coordinates, with errors of log-transformed data about 1/3 as high for the α-stable model.

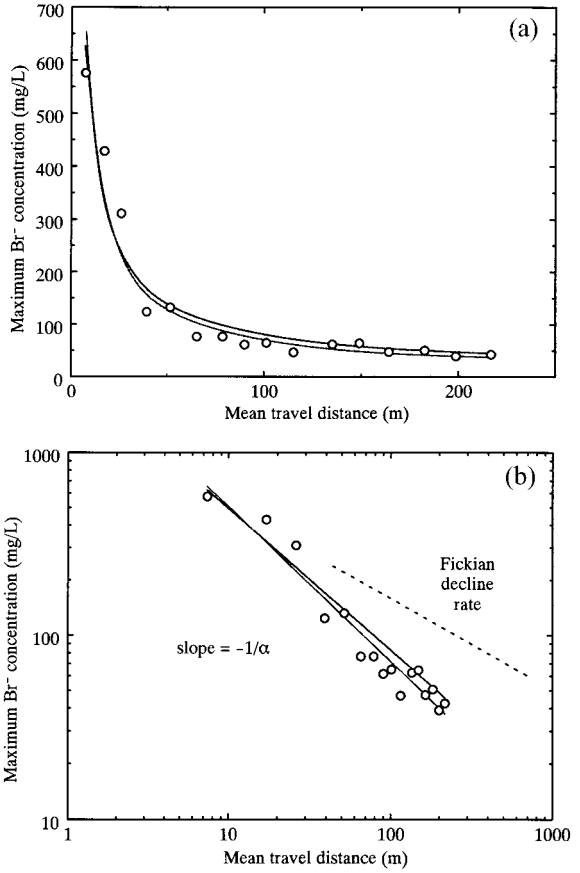

Figure 10. Maximum measured bromide concentrations in each sampling event: (a) linear coordinates and (b) log-log coordinates. The theoretical concentration decline should follow t^{-1}/α. Minimizing squared errors of untransformed data gives $\alpha = 1.3$, while minimizing squared errors of log data gives $\alpha = 1.2$.

predicted by the fractional and Fickian approaches is only realized at much later times, when the measured variance of an α-stable plume continues to grow at a nonlinear rate. Only after transformation to log-log coordinates does the fractional approach show some advantage (Figures 8b and 9b). The plots of estimated variance versus either time or $\bar{x}$ have different slopes owing to the fact that the mean velocity changed subtly throughout the test [*Garabedian et al*., 1991]. Estimates of α range from 1.65, which minimizes the data residuals after log transformation of variance versus $\bar{x}$, to 1.8, which minimizes residuals of untransformed data. We investigate both solutions.

One check of the ergodicity of the transport process is the decline rate of the concentration within some fixed portion of the plume. Since the fundamental solutions of the local ADE and the fractional ADE are densities, the height of the density (the concentration measured along the plume core) should decline at the same rate that the density grows in space. However, the rate of peak concentration decline is much more rapid than either the traditional or fractional ADEs predict (Figure 10). This suggests that (1) the calculation of plume variance is strongly influenced by detection limits, underestimating the variance (plotted in Figures 8 and 9) more strongly at later times; (2) a significant mass of bromide is partitioning into an immobile phase; (3) plume dilution is greater at later time, or (4) a temporally nonlocal governing process is at work.

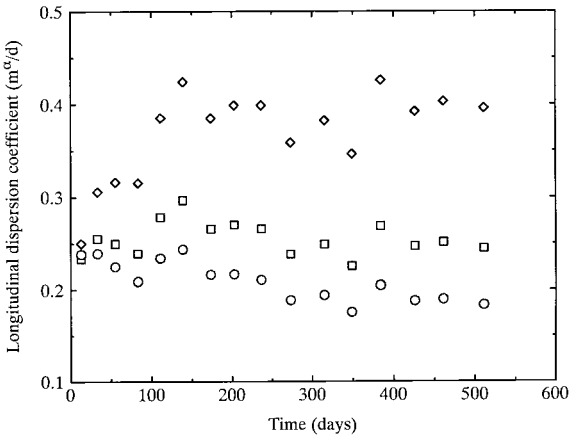

Figure 11. Estimated longitudinal dispersion coefficients for $\alpha = 2$ (diamonds), $\alpha = 1.8$ (squares), and $\alpha = 1.65$ (circles) estimated by equation (4). Early plume data give $\mathcal{D} \approx 0.25$ for $\alpha = 1.8$ and $\mathcal{D} \approx 0.21$ for $\alpha = 1.65$.

Mass recovery at the Cape Cod site was generally very good with little systematic decline [*Garabedian et al*., 1991], suggesting that the first two explanations are not important. Further, the reactor ratio (the ratio of measured to maximum plume entropy assuming a Gaussian) is relatively constant at Cape Cod [*Thierrin and Kitanidis*, 1994]. This suggests that temporal nonlocality may be important and that solutions to either a local ADE or the fractional ADE will suffer similar inaccuracies. The degree to which either solution is in error is left as an open question.

The dispersion coefficient for the FADE can be obtained by generating a standard α-stable density (appendix) and plotting this density alongside the field data measured at some point in time. The lateral shift required on log-log plot is equal to $(|\cos \pi\alpha/2|\mathcal{D}t)^{1/\alpha}$. Another method recognizes that an α-stable plume is roughly Gaussian close to the center of mass [*Samorodnitsky and Taqqu*, 1994] so the early time estimates of the dispersion coefficient based on standard methods should give a reasonable estimate. Equating the Gaussian and α-stable solutions gives

$$\left(\left| \cos \frac{\pi\alpha}{2} \right| \mathcal{D}t \right)^{1/\alpha} \approx \left(\frac{1}{2} \mathrm{VAR} \right)^{1/2}, \tag{3}$$

where VAR is the measured plume variance. From this we can roughly estimate the dispersion coefficient for a fractional ADE:

$$\mathcal{D} \approx \left(\frac{\mathrm{VAR}}{2} \right)^{\alpha/2} \frac{1}{\left| \cos \dfrac{\pi\alpha}{2} \right| t}. \tag{4}$$

Estimates of the dispersion coefficient for values of $\alpha = 1.65$, 1.8, and 2 based on the estimated variance [*Garabedian, et al*. 1991] mimics the growth of the variance (Figure 11). Since these numbers are based on the elapsed time, rather than the mean travel distance, the approximate dispersion coefficients for $\alpha = 1.8$ appear the most consistent. Had we used mean travel distance and a constant velocity, the values for $\alpha = 1.65$ would be relatively constant. Since these numbers are approximations, the calculation of $\mathcal{D}$ from t using (4) will suffice. From the early data we have α, $\mathcal{D}$ doublets of 1.65, 0.21 $m^{1.65}$/d and 1.8, 0.25 $m^{1.8}$/d. *Hess et al*. [1992] used permeameter and

flowmeter K data to estimate an asymptotic longitudinal dispersivity ranging from 0.35 to 0.78 m. We use an average of 0.5 here. With a relatively steady velocity of 0.43 m/d, the K data give an asymptotic dispersion coefficient of 0.21 m^2/d for the second-order equation. *Garabedian et al.* [1991] use the plume variance data (Figure 8) to infer an asymptotic, or Fickian, a_L value of 0.96 m, or a dispersion coefficient of 0.41 m^2/d.

2.2.2 Analytic solutions. Analytic solutions have been generated using the aquifer parameters estimated in section 2.2.1. The 1-D equations are

$$\frac{\partial C}{\partial t} + v\frac{\partial C}{\partial x} - \mathcal{D}(\bar{x})\frac{\partial^2 C}{\partial x^2} = C_0 x_0 \delta(t, x) \tag{5}$$

$$\frac{\partial C}{\partial g} + v\frac{\partial C}{\partial x} - \mathcal{D}\nabla^{\alpha} C = C_0 x_0 \delta(t, x), \tag{6}$$

where $C_0 x_0 \delta(t, x)$ denotes the initial solute concentration (C_0) spread over some injection distance x_0 which is mathematically concentrated into a delta function "spike." This number is the area under all of the concentration versus distance curves and should coincide with the injected concentration times the initial size of the injected mass. We use the value in the x direction of 640 mg/L × 400 cm = 0.256 g/cm^2 estimated by *LeBlanc et al.* [1991]. We have used the notation ∇^{α} to denote a symmetric fractional-order operator ($p = 0$), which is also known as the Riesz potential [*Samko et al.*, 1993]. In both equations, $v = 0.43$ m/d.

One measure of the predictive ability of the various methods is the shape of the fundamental solutions. If the α-stable solution to (6) provides a fair representation of the plume, one would also expect to see heavy tails [e.g., *Benson et al.*, 2000]. The Cape Cod data were not collected with this type of analysis in mind, so most MLSs were not sampled if the concentration was thought to be near the background concentration of ~0.01 mg/L. The sampling period at 349 days is an exception to this general rule, as many MLSs behind, and several ahead of, the main plume body were sampled and analyzed (Figure 12). The maximum concentration measured in vertical planes roughly perpendicular to flow (the core of the plume) are shown in the plot. The plotted data represent corrected concentrations in excess of the background of roughly 0.01 mg/L [*Garabedian et al.*, 1991]. To examine the tail characteristics, the concentrations measured at this time are also plotted on a log axis (Figure 12b). Note that four MLS did not show Br^- above background concentrations (plotted at 0.01 mg/L). Each of these points was surrounded in the forward and backward directions by at least two concentrations above background.

Analytic solutions of the fractional ADE, using values of α and $\mathcal{D}$ estimated from the first several plume measurements, show good agreement with data measured on day 349 (Figure 12a). The ADE with an asymptotic value of $\mathcal{D} = 0.21$ (an average of theoretical predictions from permeameter and flowmeter K data [see *Hess et al.*, 1992]) underpredicts total spread. A best fit Gaussian with a variance matched to the measured data has a similar shape to the fractional solutions (Figure 12a). This solution represents a value of $\mathcal{D} = 0.4$. The Fickian model underpredicts the concentrations of Br^- on the trailing (well-sampled) edge of the plume (Figure 12b). The fractional solution is typically within an order of magnitude, although the Fickian model fits the data more closely than the fractional ADE between the tails and the peak. Notable on this plot is the concave-upward shape of both the data and the α-stable solution tails. No effort was made to iteratively fit the α-stable solutions to the measured data. The Fickian solution underpredicts concentrations and arrival speed of the leading edge about as much as the fractional ADE overpredicts the same. *Benson* [1998] also shows that various averages of the MLSs perpendicular to the flow direction have a similar shape as these concentration maxima data. The averages imply that samples taken from wells screened across larger aquifer thicknesses will also show the same plume tailing on the leading and trailing edges.

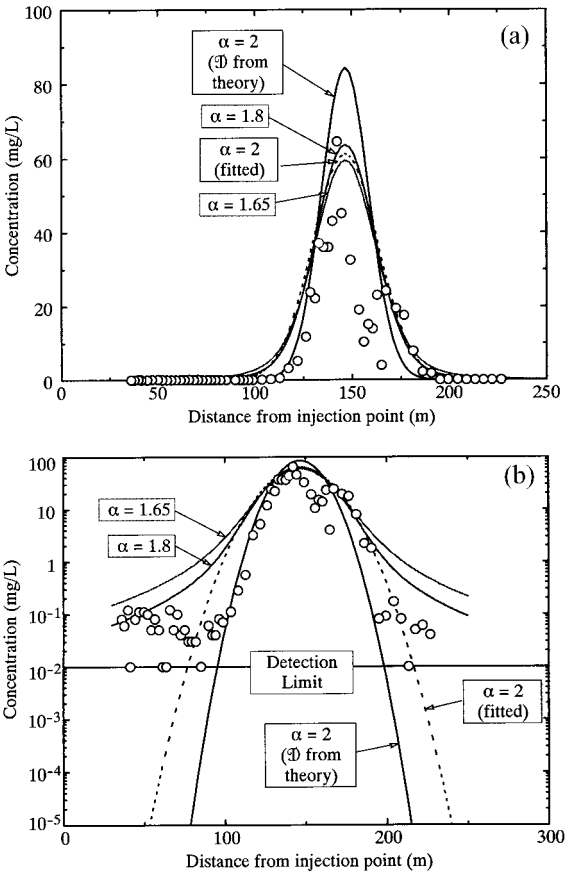

Figure 12. Predicted (solid lines) and measured (symbols) plume profile at 349 days: (a) real axes and (b) semilog axes. Concentration refers to concentration above background along the plume core. Dashed line indicates best fit Gaussian.

Solutions to (5) using the asymptotic dispersivity and to (6) using $\alpha = 1.8$ and $\mathcal{D} = 0.25$ for six other sampling rounds are very similar (Figure 13). Because the value of α is very close to 2 for the Cape Cod site, nearly indistinguishable fits (except for the tails) can be achieved at any time period by adjusting the dispersivity in the second-order equation. The curves for an asymptotic dispersivity are shown to highlight the difference on the fractional approach, which has more rapid rates of peak concentration decline and plume growth than a Fickian plume. Also shown are the solutions for $\alpha = 1.65$ and $\mathcal{D} = 0.21$ at the first and last time step, showing even more rapid growth.

3. Discussion

The fractional ADE (1) is the governing equation of all 1-D stable random walks [*Meerschaert et al.*, 1999]. If the walks are not heavy-tailed (i.e., have finite variance), then the classical central limit theorem gives $\alpha = 2$ [*Bhattacharya and Gupta*, 1990]. Walks that fit a heavy-tailed probability distribution

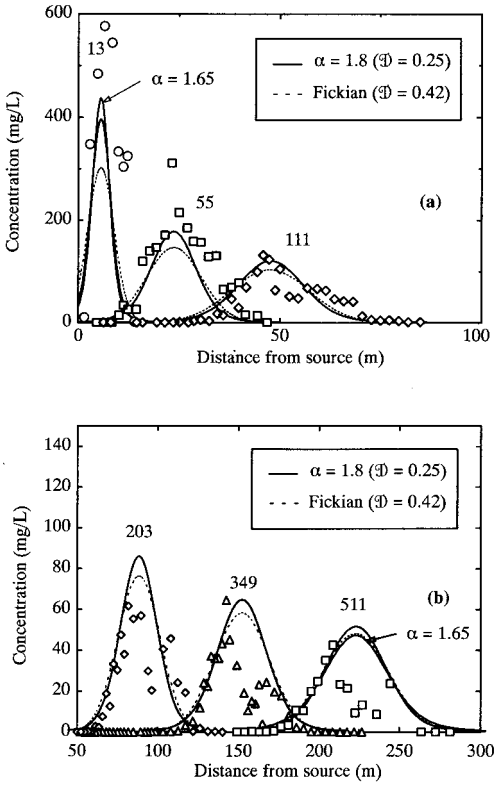

Figure 13. Analytic models of the Cape Cod plume in one dimension: (a) early time and (b) late time. Symbols are maximum concentrations measured along plume centerline. Unless otherwise noted, solid lines are solutions to fractional ADE using $\alpha = 1.8$ and $\mathcal{D} = 0.25$ m$^{1.8}$/d. Dashed lines are Fickian using asymptotic $\mathcal{D} = 0.42$ m^2/d. Sample times are shown above peaks.

(e.g., power law with index $\alpha < 2$) have infinite variance and imply a fractional equation of order α [*Meerschaert et al*., 1999]. *Benson et al*. [2000] show that a highly heterogeneous site fits this infinite variance model. The laboratory-scale sandbox and the Cape Cod aquifer are less likely candidates because of their relative homogeneity. Yet the breakthrough data in both cases are heavy-tailed and spread faster than Boltzmann scaling for most, if not all, of the plume history. These experiments indicate that a fractional-order equation is a useful predictive tool that is at least as accurate as a local, second-order equation with scale-dependent dispersivity.

The number of parameters required in a governing equation for early and late time plume predictions remains equal to or less than that needed for the traditional ADE. The dispersion coefficient is a constant, rather than a function of time or mean travel distance [*Dagan*, 1988; *Neuman and Zhang*, 1990; *Rajaram and Gelhar*, 1995], reducing the number by one. This is replaced by the order of differentiation in (1). To get skewness (and tailing with a local ADE), another parameter is needed for any order equation: p for the fractional ADE and a mass transfer rate coefficient for mobile/immobile formulations. Since two-phase mobile/immobile solutions produce exponential, not power law tails, it is not well suited to the sandbox data. *Haggerty et al*. [1998] have shown that an infinite number of immobile phases can produce power law tailing, if the rate coefficient probability distribution has a power law tail. This is conceptually similar to the fractional ADE, which explicitly dictates that very slow particle motions have a much higher probability than the Gaussian can allow. An open question is the exact nature of the overlap between a fractional ADE and the infinite immobile phase model of *Haggerty et al*. [1998].

These analyses are purely heuristic. A direct link between the order of the governing equation and the hydraulic properties of the sandbox and Cape Cod aquifer remains to be shown. However, since the fractional ADE uses constant parameters, their values may be estimated from several early measurements of the plume. Knowledge of the K autocorrelation properties is not needed for long-term predictions. This may be financially beneficial, since plume concentrations are often measured at contaminated sites while the K structure is not.

4. Conclusions

The fractional ADE is compatible with observations of plumes in the laboratory and the field. It predicts power law, faster than linear scaling of the apparent plume variance. The fundamental solutions are α-stable densities with heavy tails that may arise from hydraulics alone. The parameters in the equation can be calculated from early time plume growth or breakthrough curve data. While *Benson et al*. [2000] indicate that the parameters can also be discerned from the K distribution at highly heterogeneous sites, this type of analysis has not yet been applied to the relatively homogeneous sandbox and Cape Cod aquifer. Tracer data show that a predictive equation valid over a wide range of time and distance scales can be found in the absence of aquifer K data.

Building a homogeneous sandbox is clearly a difficult endeavor. Deviations from the homogeneous ideal were manifest in the heavy (power law) tailed 1-D tracer tests. The very fast and very slow tracer excursions also cause the plume width to grow faster than by $t^{1/2}$. The number of effective parameters needed to model a plume's behavior is equal to, or less than, that required by a local, second-order equation. While the reduction of $\mathcal{D}(\bar{x})$ to a constant $\mathcal{D}$ reduces the number of parameters by one, the fitted order of differentiation restores the amount of information needed in the governing equation. To get skewness, one can use a mobile/immobile rate coefficient or the fractional ADE's skewness parameter p. This parameter allows the heavy trailing edge similar to mobile/immobile solutions and will also allow heavier leading edges such as that found in the Macro Dispersion Experiment (MADE) tracer tests at the Columbus Air Force Base in Mississippi [*Benson et al*., 2000]. We have not investigated the skewness achievable by nonlocal methods [e.g., *Deng et al*., 1993].

Early plume data at Cape Cod indicate an order of differentiation α of the order of 1.65 to 1.8. While the fits of the Gaussian and α-stable solutions are about the same in the Cape Cod bromide plume at 349 days, the Gaussian solution underpredicts concentration and speed of the leading edge, while the α-stable solution overpredicts the same. The differences in the tail concentrations predicted by the Gaussian versus α-stable solutions span many orders of magnitude, especially at very low concentration and large distances. Differences between $\alpha = 1.65$ and 1.8 solutions are less pronounced.

Appendix

Fractional derivatives of a function with domain $(-\infty, \infty)$ can be defined several ways. We use a scaled combination of two operators defined [*Samko et al*., 1993; *Debnath*, 1995; *Benson et*

al., 2000] by extending the well-known action of Fourier transform on integer derivatives $\mathcal{F}[(d^n/dx^n)f(x)] = (ik)^n\hat{f}(k)$ to rational order: $\mathcal{F}[(d^\alpha/dx^\alpha)f(x)] = (ik)^\alpha\hat{f}(k)$, where $f(x)$ and $\hat{f}(k)$ are Fourier transform pairs. If the derivative is taken with respect to $-x$, we substitute $-k$ for k:

$$\mathcal{F}\left[\frac{d^\alpha}{d(-x)^\alpha}f(x)\right] = (-ik)^\alpha\hat{f}(k).$$

By inverse transform [*Samko et al*., 1993; *Benson et al*., 1999], one finds that these fractional derivatives have the 1-D representations:

$$\frac{d^\alpha f(x)}{dx^\alpha} = \frac{1}{\Gamma(n-\alpha)}\frac{d^n}{dx^n}\int_{-\infty}^{x}(x-\xi)^{n-1-\alpha}f(x)\,d\xi \tag{A1}$$

$$\frac{d^\alpha f(x)}{d(-x)^\alpha} = \frac{(-1)^n}{\Gamma(n-\alpha)}\frac{d^n}{dx^n}\int_{x}^{\infty}(\xi-x)^{n-1-\alpha}f(x)\,d\xi \tag{A2}$$

with the single shorthand notation [*Samko et al*., 1993]:

$$D_{\pm}^{\alpha}f(x) = \frac{(\pm 1)^n}{\Gamma(n-\alpha)}\frac{d^n}{dx^n}\int_{0}^{\infty}\xi^{n-\alpha-1}f(x\mp\xi)\,d\xi, \tag{A3}$$

where $\Gamma(\ )$ is the Gamma function and n is the smallest integer larger than α. The Green function solution to (1), representing an instantaneous pulse source, is an α-stable density denoted $f_{\alpha\beta\sigma\delta}(x)$, where α is the index of stability, β is the skewness, σ is the scale, and δ is the shift. A standard density has $\sigma = 1$ and $\delta = 0$. A general density is related to the standard by $f_{\alpha\beta\sigma\delta}(x) = \sigma^{-1}f_{\alpha\beta10}((x-\delta)/\sigma)$. The solution to the 1-D fractional ADE has $\delta = vt$ and $\sigma = [|\cos(\pi\alpha/2)|\mathcal{D}t]^{1/\alpha}$ [*Benson*, 1998]. Given v and $\mathcal{D}$, one can specify any x and t and find the standard density for the argument $(x - vt)/[|\cos(\pi\alpha/2)|\mathcal{D}t]^{1/\alpha}$. The canonical forms of the density assume many different definitions of a skewness parameter. Our choice of p is related to *Samorodnitsky and Taqqu*'s [1994] common skewness parameter (β) by $\beta = 2p - 1$. A standard density can be found by integrating the expression [*Benson*, 1998]

$$f_{\alpha\beta10}(x) = \frac{|cx|^{1/(\alpha-1)}\alpha c}{c|1-\alpha|}\cdot\int_{-\theta}^{1}U_\alpha(\phi,\theta)\exp[-|cx|^{\alpha/(\alpha-1)}U(\phi,\theta)]\,d\phi, \tag{A4}$$

where

$$c = \{1 + [\beta\tan(\pi\alpha/2)]^2\}^{-1/2\alpha},$$

$$\theta = \frac{2}{\pi\alpha}\tan^{-1}(\beta\tan(\pi\alpha/2)),$$

$$U_\alpha(\phi,\theta) = \left(\frac{\sin\frac{\pi}{2}\alpha(\phi+\theta)}{\cos\frac{\pi}{2}\phi}\right)^{\alpha/(1-\alpha)},$$

or by *Feller*'s [1971] series (for $1 < \alpha \le 2$):

$$f_{\alpha\gamma10}(x) = \frac{1}{\pi x}\sum_{k=0}^{\infty}\frac{\Gamma(k\alpha^{-1}+1)}{k!}(-x)^k\sin\frac{\pi k}{2\alpha}(\gamma-\alpha), \tag{A5}$$

where Feller's skewness parameter γ is obtained from β by [*Samorodnitsky and Taqqu*, 1994]

$$\gamma = \frac{2}{\pi}\arctan[\beta\tan(\pi(\alpha-2)/2)]. \tag{A6}$$

For symmetric densities, setting $\beta = \gamma = 0$ in (A5) yields a formula that converges rapidly even for large arguments. The symmetric standard density for $1 < \alpha \le 2$ is given by the series

$$f_{\alpha010}(x) = \frac{1}{\pi}\sum_{k=0}^{\infty}\frac{(-1)^k}{(2k+1)!}\Gamma\left(\frac{2k+1}{\alpha}+1\right)x^{2k}. \tag{A7}$$

The integral expression was incorporated into FORTRAN codes (cvt.f and cvx.f [*Benson*, 1998, Appendix I]) that generate expected concentration versus time (at a point in space) or distance (at a specific time).

Acknowledgments. D.A.B. received partial support from the U.S. Department of Energy, Basic Energy Sciences grant DE-FG03-98ER14885. We thank Kathryn Hess with the USGS for providing the Cape Cod data. We also thank J. H. Cushman, S. P. Neuman, and an anonymous reviewer for their criticism.

References

Benson, D. A., The fractional advection-dispersion equation: Development and application, Ph.D. thesis, Univ. of Nev., Reno, 1998.

Benson, D. A., R. Schumer, M. M. Meerschaert, and S. W. Wheatcraft, Fractional dispersion, Lévy flights, and the MADE tracer tests, *Transp. Porous Media*, in press, 2000.

Berkowitz, B., and H. Scher, On characterization of anomalous dispersion in porous and fractured media, *Water Resour. Res*., *31*(6), 1461–1466, 1995.

Berkowitz, B., and H. Scher, Theory of anomalous chemical transport in random fracture networks, *Phys. Rev. E*, *57*(5), 5858–5869, 1998.

Bhattacharya, R., and V. K. Gupta, Application of central limit theorems to solute transport in saturated porous media: From kinetic to field scales, in *Dynamics of Fluids in Hierarchical Porous Media*, edited by J. H. Cushman, pp. 61–96, Academic, San Diego, Calif., 1990.

Brusseau, M. L., R. E. Jessup, and P. S. C. Rao, Modeling the transport of solutes influenced by multi-process nonequilibrium, *Water Resour. Res*., *25*(9), 1971–1988, 1989.

Burns, E., Results of 2-dimensional sandbox experiments: Longitudinal dispersivity determination and seawater intrusion of coastal aquifers, Master's thesis, Univ. of Nev., Reno, 1996.

Chaves, A. S., A fractional diffusion equation to describe Lévy flights, *Phys. Lett. A*, *239*, 13–16, 1998.

Coats, K. H., and B. D. Smith, Dead-end pore volume and dispersion in porous media, *Soc. Pet. Eng. J*., *4*, 73–84, 1964.

Compte, A., Stochastic foundations of fractional dynamics, *Phys. Rev. E*, *53*(4), 4191–4193, 1996.

Cushman, J. H., X. Hu, and T. R. Ginn, Nonequilibrium statistical mechanics of preasymptotic dispersion, *J. Stat. Phys*., *75*(5/6), 859–878, 1994.

Dagan, G., Time-dependent macrodispersion for solute transport in anisotropic heterogeneous aquifers, *Water Resour. Res*., *24*(9), 1491–1500, 1988.

Debnath, L., *Integral Transforms and Their Applications*, CRC Press, Boca Raton, Fla., 1995.

de Josselin de Jong, G., Longitudinal and transverse diffusion in granular deposits, *Eos Trans. AGU*, *39*(1), 67–74, 1958.

Deng, F.-W., J. H. Cushman, and J. W. Delleur, A fast Fourier transform stochastic analysis of the contaminant transport problem, *Water Resour. Res*., *29*(9), 3241–3247, 1993.

Feller, W., *An Introduction to Probability Theory and Its Applications*, vol. II, 2nd ed., John Wiley, New York, 1971.

Garabedian, S. P., D. R. LeBlanc, L. W. Gelhar, and M. A. Celia, Large-scale natural gradient tracer test in sand and gravel, Cape Cod, Massachusetts, 2, Analysis of spatial moments for a nonreactive tracer, *Water Resour. Res*., *27*(5), 911–924, 1991.

Giona, M., and H. E. Roman, A theory of transport phenomena in disordered systems, *Chem. Eng. J*., *49*, 1–10, 1992.

Gorenflo, R., and F. Mainardi, Fractional calculus and stable probability distributions, *Arch. Mech*., *50*(3), 377–388, 1998.

Haggerty, R., and S. M. Gorelick, Multiple-rate mass transfer for modeling diffusion and surface reactions in media with pore-scale heterogeneity, *Water Resour. Res*., *31*(10), 2383–2400, 1995.

Haggerty, R., S. A. McKenna, and L. Meigs, Power-law behavior of groundwater tracer test breakthrough curves at late time, *Eos Trans. AGU*, *79*(45), Fall Meet. Suppl., F294, 1998.

Henry, H. R., Effects of dispersion on salt encroachment in coastal aquifers, in *Sea Water in Coastal Aquifers*, *U.S. Geol. Surv. Water Supply Pap*., *1613-C*, 70–84, 1964.

Hess, K. M., S. H. Wolf, and M. A. Celia, Large-scale natural gradient tracer test in sand and gravel, Cape Cod, Massachusetts, 3, Hydraulic conductivity variability and calculated dispersivities, *Water Resour. Res*., *28*(8), 2011–2027, 1992.

Kapoor, V., and L. W. Gelhar, Transport in three-dimensionally heterogeneous aquifers, 2, Predictions and observations of concentration fluctuations, *Water Resour. Res*., *30*(6), 1789–1801, 1994.

LeBlanc, D. R., Garabedian, S. P., K. M. Hess, L. W. Gelhar, R. D. Quadri, K. G. Stollenwerk, and W. W. Wood, Large-scale natural gradient tracer test in sand and gravel, Cape Cod, Massachusetts, 1, Experimental design and observed tracer movement, *Water Resour. Res*., *27*(5), 895–910, 1991.

Lévy, P., *Théorie de l'Addition des Variables Aléatoires*, Gauthier-Villars, Paris, 1937.

Li, L., D. A. Barry, P. J. Culligan-Hensley, and K. Bajracharya, Mass transfer in soils with local stratification of hydraulic conductivity, *Water Resour. Res*., *30*(11), 2891–2900. 1994.

Meerschaert, M. M., D. A. Benson, and B. Bäumer, Multidimensional advection and fractional dispersion, *Phys. Rev. E*, *59*(5), 5026–5028, 1999.

Montroll, E. W., and G. H. Weiss, Random walks on lattices, II, *J. Math. Phys*., *6*(2), 167–181, 1965.

Neuman, S. P., Eulerian-Langrangian theory of transport in space-time nonstationary velocity fields: Exact nonlocal formalism by conditional moments and weak approximation, *Water Resour. Res*., *29*(3), 633–645, 1993.

Neuman, S. P., and Y.-K. Zhang, A quasi-linear theory of non-Fickian and Fickian subsurface dispersion, 1, Theoretical analysis with application to isotropic media, *Water Resour. Res*., *26*(5), 887–902, 1990.

Painter, S., V. Cvetkovic, and J.-O. Selroos, Transport and retension in fractured rock: Consequences of a power-law distribution for fracture lengths, *Phys. Rev. E*, *57*(6), 6917–6922, 1998.

Pickens, J. F., and G. E. Grisak, Scale-dependent dispersion in a stratified granular aquifer, *Water Resour. Res*., *17*(4), 1191–1211, 1981.

Rajaram, H., and L. W. Gelhar, Plume-scale dependent dispersion in aquifers with a wide range of scales of heterogeneity, *Water Resour. Res*., *31*(10), 2469–2482, 1995.

Saichev, A. I., and G. M. Zaslavsky, Fractional kinetic equations: Solutions and applications, *Chaos*, *7*(4), 753–764, 1997.

Samko, S. G., A. A. Kilbas, and O. I. Marichev, *Fractional Integrals and Derivatives: Theory and Applications*, Gordon and Breach, Newark, N. J., 1993.

Samorodnitsky, G., and M. S. Taqqu, *Stable Non-Gaussian Random Processes*, Chapman and Hall, New York, 1994.

Taylor, Sir G. I., Dispersion of soluble matter in solvent flowing slowly through a tube, *Proc. R. Soc. London*, *Ser. A*, *219*, 186–203, 1953.

Thierrin, J., and P. K. Kitanidis, Solute dilution at the Borden and Cape Cod groundwater tracer tests, *Water Resour. Res*., *30*(11), 2883–2890, 1994.

van Genuchten, M. T., and P. J. Wierenga, Mass transfer studies in sorbing porous media, I, Analytical solutions, *Soil Sci. Soc. Am. J*., *40*, 473–481, 1976.

D. A. Benson, Desert Research Institute, Water Resources Center, 2215 Raggio Parkway, Reno, NV 89512-1095. (debenson@dri.edu)

M. M. Meerschaert, Department of Mathematics, University of Nevada, Reno, NV 89557.

S. W. Wheatcraft, Department of Geologic Sciences, University of Nevada, Reno, NV 89557.

(Received September 24, 1999; revised January 10, 2000; accepted February 11, 2000.)